ЖЭТФ, 2025, том 168, вып. 3 (9), стр. 401–413 

# ON THE THEORY OF HOMOGENEOUS NUCLEATION OF CRYSTALS FROM MELTS

***M. S. Veshchunov****

*Nuclear Safety Institute (IBRAE), Russian Academy of Sciences*
*115191, Moscow, Russia*

Received June 10, 2025,
revised version June 10, 2025
Accepted for publication June 16, 2025

A new model for the kinetics of homogeneous nucleation of crystals from melts is developed in the framework of classical nucleation theory. The traditional approach considering the mechanism of mass transfer from the melt to nucleated particles by random attachment of atoms at the interface, which is valid for crystals with atomically rough interface, is modified in application to faceted crystalline particles with atomically smooth interface, whose growth is controlled by two-dimensional nucleation of terraces of monoatomic height on the crystal faces. The new model demonstrates a strong suppression of the nucleation rate compared to the traditional approach.

**DOI:** 10.7868/S3034641X25100134

## 1. INTRODUCTION

Experience shows that in supercooled or supersaturated liquids crystals may not appear for a long time. Molten specimens of many metals can be supercooled by several hundred degrees below the melting point $T_0$, down to temperatures of 0.7–0.8 $T_0$. The cause of such stability in metastable systems is that the formation of small nuclei of the stable crystal phase is an activated process that may be extremely slow [1,2]. Nevertheless, when it occurs, the subsequent growth process is rapid. This may explain why there is a scarcity of experimental data on crystal nucleation.

The classical theory of homogeneous nucleation [3–5] is commonly used to estimate the height of the nucleation barrier and to predict the rate of crystal nucleation. In the simplest isotropic approximation (commonly used), the equilibrium shape of a nucleus is a sphere, and the process by which crystal nuclei are formed is similar to that for the formation of liquid drops in a supercooled vapour, or drops of one liquid in another during liquation. For nuclei with faceted crystal structure, the isotropic approximation is slightly modified by recalculating the volume and surface of the nucleus for a more realistic geometry and using the 'effective' surface tension averaged over different faces. This enables to evaluate the activation energy of nucleation and thus the exponential (thermodynamic) factor of the nucleation rate [1, 2].

The arrival (or forward reaction) rate of single atoms (or molecules) to the critical nucleus, which determines a pre-exponential kinetic factor of the nucleation rate, for the nucleation of crystals from vapour is calculated similarly to nucleation of liquid droplets from vapour in the framework of the kinetic theory of gases (as the collision rate of gas atoms with the critical cluster surface). The procedure for calculating rate constants for nucleation from liquids is less obvious and is usually based on the approach of Turnbull and Fischer [6], who assumed that when a single atom or molecule is added or removed in a cluster, the system passes through a configuration (activated complex) that is higher in energy than the initial or new state and determines the activation energy for atoms hopping to the cluster surface. For practical applications, the jump frequency is generally taken to be the same as that governing bulk diffusion [1]. This approach is consistent with the classical nucleation theory, in which the arrival rate is related to the growth mechanism of a particle (see details below in Section 4), but only in the case of liquid droplets or crystals with atomically rough surfaces, whose growth is governed by random attachment of atoms at the interface. However, in the case of crystals with atomically smooth surfaces the situation may be essentially different.

* E-mail: msvesh@gmail.com

Indeed, it is well known since the paper of Burton, Cabrera and Frank [7] that the growth rate of a given face for a perfect crystal must show a discontinuity at its roughening temperature. At temperatures above the roughening transition, the growth is controlled by random attachment of atoms at the interface [6] and is relatively fast, whereas below the roughening transition, the growth is controlled by two-dimensional (2D) nucleation of terraces of monoatomic height on the crystal faces and is correspondingly strongly suppressed. As a consequence of this change in the growth mechanism the crystal morphology changes. At elevated temperatures, the rough faces grow rapidly maintaining the quasi-spherical shape of the crystal; however, at temperatures below their roughening transition, the growth shape becomes constrained by the faces with slow growth rates.

This change of behaviour has been studied for crystal growth in both vapours [8, 9] and melts [10, 11]. In particular, in the case of metallic crystals precipitating from melts, it was observed that towards the high temperatures, the melting point in many materials is reached before the roughening transition of the plane facets [12]. This makes logical to assume that clusters nucleating from melts over a wide range of temperatures will have atomically smooth surfaces.

Nucleation is a dynamical process usually occurring on very small time and length scales (nanoseconds and nanometres, respectively). Thus, obtaining the necessary spatial and temporal resolutions is a tough technical challenge, and experimental methods that can detect nucleation and the formation of the crystal (predominantly by means of optical microscopy) do not provide any microscopic detail on the structure of nucleated crystalline phase. For this reason, atomistic computer simulations can provide unique insights into the microscopic aspects of crystallisation [13].

For instance, the solidification of molybdenum nanoparticles from liquid droplets at different cooling rates was performed by molecular dynamics (MD) simulation [14]. The range of nanoparticle structures obtained by cooling liquid droplets was examined by direct observation of the atomic configuration. At the lowest cooling rate, $2 \cdot 10^{10}$ K/s, a nanoparticle consisting of a bcc single crystal with faceted surface was formed at all sizes above ≈130 atoms (or radii above ≈0.8 nm) as a result of the phase transition from the liquid phase to the bcc phase. On the other hand, at the highest cooling rate, $10^{13}$ K/s, a glassy structure was formed in the nanoparticles, in which the disordered structure of the liquid was preserved due to the rapid quenching.

Similarly, MD simulations for homogeneous nucleation in aluminium melt [15] showed that at 500 K the solid–liquid interfacial energy has large orientation dependence and the formation of faceted crystalline nuclei is expected. Also, because there is less effect of solid–liquid interfacial energy anisotropy at higher temperatures, each nucleus can almost reach a spherical shape (at 700 K in simulations).

Furthermore, results from MD simulations of crystal nucleation in molten NaCl at moderate supercooling showed that the critical nucleus formed during the nucleation process has the rock salt crystal structure of bulk NaCl and is clearly faceted [16]. In particular, it was concluded that homogeneous crystal nucleation in molten NaCl does not proceed via an intermediate metastable phase, in contrast to results from MD simulations of NaCl nucleation from aqueous solution (e. g., [17]), where the early stage nucleus was a loosely ordered arrangement of ions retaining a significant amount of water, followed by a slow removal of water as the cluster grows and evolves towards its stable rock salt structure. Comparison of these simulation results may explain the difference in the two nucleation mechanisms (the one-step mechanism by direct nucleation of crystalline nuclei in NaCl melt, and the two-step mechanism by preliminary formation of dense disordered clusters in NaCl aqueous solution) by the strong influence of water molecules on the structure of relatively small clusters (revealed in simulations [17]).

As noted in [16], the simulation results of crystal nucleation in molten NaCl are in qualitative agreement with visual observations of crystallisation in alkali halide droplets by Buckle and Ubbelohde [18], who detected the presence of 'twinkling' crystalline nuclei by illuminating condensed salt vapours with a narrow beam of nearly parallel light. Analysing the results of their tests, Buckle and Ubbelohde concluded that classical nucleation theory should be modified to take into account the three-dimensional crystal structure of alkali halide nuclei, which are bounded by perfectly close-packed planes (up to the melting point) and whose growth can only occur by repeated 2D nucleation of fresh surface layers. This deduction may explain the large discrepancies between the results of MD calculations [16] and experimental nucleation rates when traditional nucleation theory (assuming atomically rough cluster surfaces) was used to extrapolate the calculation results to the milder supercooling probed by the actual measurements.

Such a modification of the nucleation theory will be carried out in the present study, demonstrating a strong suppression of the nucleation rate of crystallites with

atomically smooth faces compared to the results of traditional models considering atomically rough surfaces.

## 2. NUCLEATION AND GROWTH OF TERRACES

The classical nucleation theory [3, 4], in which nuclei of the new phase of the critical size are assumed to be in equilibrium with the transformed phase, yields an expression for the nucleation rate,

$$\dot{N} = N^* \omega^*, \tag{1}$$

where $\omega^*$ is the rate at which monomers (atoms or molecules) of volume $\Omega$ arrive at the critical nucleus (cluster) of radius $R^*$, consisting of

$$n^* \approx \frac{4\pi R^{*3}}{3\Omega}$$

monomers, from the metastable phase, and $N^*$ is the number density of the critical nuclei, calculated as

$$N^* = N_1 \exp\left(-\frac{\Delta G^*}{kT}\right), \tag{2}$$

where $N_1$ is the number density of monomers in the metastable phase, $\Delta G^* \equiv \Delta G\,(R^*)$ is the free energy of formation of the critical nucleus. Zeldovich [5] refined this treatment to account for depletion of critical nuclei in the non-equilibrium situation, yielding

$$\dot{N} = Z\omega^* N_1 \exp\left(-\frac{\Delta G^*}{kT}\right), \tag{3}$$

where $Z$ is the non-equilibrium Zeldovich factor,

$$Z = \left[-\frac{1}{2\pi kT}\left(\frac{d^2\Delta G(n)}{dn^2}\right)_{n=n^*}\right]^{1/2}. \tag{4}$$

### 2.1. Nucleation of terraces on a smooth surface

The rate theory for formation of a two-dimensional nucleus on a perfect crystal plane from vapour was developed by Pound et al. [19], who modified the classical expression for $N^*$, Eq. (2), considering $N_1 = \overline{c}_a a\Omega^{-1}$ (where $a$ is the monolayer thickness) as the number density of adsorbed vapour atoms (adatoms) with the dimensionless surface concentration $\overline{c}_a \ll 1$ in equilibrium with the supersaturated vapour phase of partial pressure $p \geq p_0$, or $\alpha = p/p_0 \geq 1$, where $p_0$ is the saturation pressure and $\alpha$ is the supersaturation ratio. In this approach, $N_1$ is determined from the condition of equal chemical potentials of adatoms and vapour atoms,

$$\mu_a = kT\ln\left(\frac{\overline{c}_a}{c_a^*}\right) = kT\ln\left(\frac{p}{p_0}\right),$$

or

$$\frac{\overline{c}_a}{c_a^*} = \frac{p}{p_0} = \alpha,$$

where $c_a^*$ is the saturation concentration of adatoms.

Accordingly, the formation free energy of a nucleus of radius $\rho$ is calculated as

$$\Delta G(\rho) = -\frac{\pi\rho^2}{s}\left(\mu_a - \mu_a^{'}\right) + 2\pi\rho\lambda = -\frac{\pi\rho^2 a}{\Omega}kT\ln\alpha + 2\pi\rho\lambda, \tag{5}$$

where $\lambda$ is the energy per unit length of monomolecular edge, $s \approx \Omega/a$ is the specific area of an adatom, and

$$\Delta\mu_a = \mu_a - \mu_a^{'} = kT\ln\left(\frac{\overline{c}_a}{c_a^*}\right) = kT\ln\alpha$$

is the difference of the chemical potentials in the two phases of adatoms (surface lattice gas and dense phase forming a monoatomic layer), which determines the critical nucleus radius

$$\rho^* = \frac{\lambda s}{kT\ln\alpha},$$

evaluated from the condition

$$\frac{d\Delta G(\rho)}{d\rho} = 0.$$

Respectively, the formation free energy of the critical nucleus is equal to

$$\Delta G^* = \Delta G\,(\rho^*) = \lambda\pi\rho^* = \frac{\pi\lambda^2 s}{kT\ln\alpha}.$$

In terms of the number $n$ of adatoms forming a nucleus of radius

$$\rho = \left(\frac{n\Omega}{\pi a}\right)^{1/2},$$

Eq. (5) can be represented in the form

$$\Delta G(n) = -n\left(\mu_a - \mu_a^{'}\right) + 2\lambda\left(\frac{\pi\Omega}{a}\right)^{1/2} n^{1/2} = -nkT\ln\alpha + 2\lambda\left(\frac{\pi\Omega}{a}\right)^{1/2} n^{1/2}. \tag{6}$$

This approach was further refined by Hirth [20], who calculated the non-equilibrium Zeldovich factor for a disc-shaped nucleus on the surface from Eq. (4) as

$$Z = \left(\frac{\Delta G^*}{4\pi kTn^{*2}}\right)^{1/2}, \tag{7}$$

where

$$n^* \approx \frac{\pi {\rho^*}^2 a}{\Omega}$$

is the number of adatoms in the critical nucleus.

The rate at which adatoms join the critical nuclei was estimated as

$$\omega^* \approx \frac{1}{4a} 2\pi\rho^* \overline{c}_a \nu,$$

given by the product of the number $\approx 2\pi\rho^*\overline{c}_a a^{-1}$ of adatoms in a position to join a critical nucleus times the frequency with which such an adatom will jump to join the nucleus,

$$\nu \approx \nu_s \exp\left(-\frac{\Delta G_{sd}}{kT}\right),$$

multiplied by the probability of jumping in the direction of the critical nucleus, equal to 1/4. Here $\nu_s$ is the vibrational frequency of adatoms, and $G_{sd}$ is assumed to be equal to the activation energy for surface diffusion; thus in terms of the surface diffusivity,

$$D_s \approx \frac{1}{4} a^2 \nu_s \exp\left(-\frac{\Delta G_{sd}}{kT}\right),$$

the arrival rate takes the form

$$\omega^* \approx 2\pi\rho^*\overline{c}_a D_s a^{-3}. \tag{8}$$

However, previous attempts to apply a simplified approach similar to Eq. (8) were criticised by Cabrera and Burton [21], who noted that this model is based on the assumption that the supersaturation is the same over the entire surface of the precipitate, which is not true if there is surface diffusion. With a more consistent approach, the growth of a single terrace on the top of a flat surface is controlled by the surface diffusion transport of adatoms, considering non-uniform distribution of adatoms around the nucleus, $c_a(r)$. For this reason, the arrival rate $\omega_a$ of adatoms to a critical terrace of radius $\rho^*$ on the interface (with a linear size $L$) is determined by the solution to the steady state diffusion problem in the surface layer of thickness $\approx a$, taking into account the evaporation of adatoms into the gas phase. This leads to the additional factor

$$\frac{a}{x_s} = \frac{a}{x_s} \sim 10^{-2} - 10^{-3}$$

in Eq. (8), where

$$x_s = (D_s \tau_s)^{1/2}$$

is the diffusion length defined as the mean displacement of an adatom during its mean life $\tau_s$ on the surface before being evaporated, as shown in the author's paper [22].

The nucleation model [19] can be modified to analyse the formation of a two-dimensional nucleus on an infinite flat interface with a melt. The adsorption of atoms at the solid-melt interface can be considered analogous to the adsorption of solute atoms at the solid-liquid interface, studied in colloidal systems (see, e. g., [23]), as the formation of point defects (adatoms) at the interface (more generally, along with other point defects, surface vacancies formed in the upper solid layer, discussed below in Sections 2 and 3). In this case, the difference in chemical potentials of atoms in liquid and solid phases is equal to

$$\mu_l - \mu_s = \Delta g = \Delta S_f \Delta T,$$

where $\Delta T = T - T_m$ is undercooling and $\Delta S_f$ is the entropy of fusion per atom; the mean surface concentration $\bar{c}_a$ is determined from the condition of equilibrium of adatoms with the melt,

$$kT \ln\left(\bar{c}_a / c_a^{(0)}\right) = \mu_l,$$

where $c_a^{(0)}(T)$ is the thermal surface concentration of adatoms, and the saturation surface concentration $c_a^*$ is determined from the condition of equilibrium of adatoms with the solid phase,

$$kT \ln\left(c_a^* / c_a^{(0)}\right) = \mu_s.$$

Therefore, the supersaturation ratio can be represented in the form

$$\alpha = \frac{\overline{c}_a}{c_a^*} = \exp\left(\frac{\Delta g}{kT}\right). \tag{9}$$

The saturation concentration $c_a^*$ also corresponds to the equilibrium between adsorbed atoms and a step of monomolecular height $a$ and of infinite length; at $\overline{c}_a > c_a^*$, the step will move (due to the diffusion influx of adatoms) until it forms a full monolayer, and at $\overline{c}_a < c_a^*$, it will move in the opposite direction until it disappears. In the case of a disk-shaped nucleus of radius $\rho$, it will grow if

$$\overline{c}_a \geq c_{a,\rho}^* = c_a^* \exp\left(\frac{\lambda s}{\rho kT}\right),$$

in accordance with the Gibbs – Kelvin equation for the equilibrium concentration $c_{a,\rho}^*$, and will shrink in the opposite case,

$$\overline{c}_a < c_a^* \exp\left(\frac{\lambda s}{\rho kT}\right).$$

Correspondingly, the radius of a critical nucleus can be calculated from the condition

$$\overline{c}_a = c_a^* \exp\left(\frac{\lambda s}{\rho^* kT}\right),$$

which obviously coincides with the above derived expression, $\rho^* = \lambda s/kT\ln\alpha$, and thus $\rho^* \to \infty$ at saturation, when $\alpha \to 0$. Therefore, the above theory [19] can be applied only to the nucleation of terraces on the surface of relatively large particles of radius $R \gg \rho^*$ (i. e., at relatively high supercoolings), and becomes inapplicable for particles of finite size.

Furthermore, for the nucleation of terraces at the interface with the melt, Eq. (8) can be simplistically re-estimated from the solution of the steady-state surface diffusion problem with the boundary condition away from the nucleus defined by the mean surface concentration $\overline{c}_a$ (sustained by the condition of equilibrium of adatoms with the melt), $c_a(L) = \overline{c}_a$, and thus determines the arrival rate with logarithmic accuracy as

$$\omega_a(\rho) \approx \frac{2\pi\overline{c}_a D_s a}{\Omega \ln\left(\frac{L}{\rho}\right)}. \tag{10}$$

This logarithmic approximation is well justified for $\rho \ll L$, but for simplicity will further be used for larger terraces as well.

More generally, the contribution of three-dimensional effects to the surface diffusion problem (more accurately accounting for the exchange of adatoms with the melt during diffusion along the surface) may also be important and thus may further modify Eq. (10). In particular, in MD simulations [24] no differences were found between the diffusion coefficients at the solid-liquid interface in the lateral and normal directions to the surface; in this case, the arrival rate should be determined from a self-consistent solution of the diffusion problem in the melt and at the interface. However, these effects will be neglected in analytical calculations, using this simplified expression for the arrival rate at the terraces, Eq. (10), but which can be corrected in the final expression for the crystal nucleation rate obtained below in Section 4, if a more accurate solution to the diffusion problem is found.

### 2.2. Nucleation of terraces on the surface of finite size particles

To describe the formation of a new monolayer terrace on the surface of finite size particles with atomically smooth surface, Eq. (5) should be additionally modified. This can be done in the commonly used isotropic approximation (discussed in Section 1), in which the nucleus is considered as a spherical particle with the 'effective' surface tension averaged over different faces, and taking into account the 'quasi-spherical' shape of faceted crystallites usually observed in the tests (see, e. g., [12]). For such geometry the differences in volume and total surface area of real and spherical particles are not very significant and in the first approximation they can be neglected (and, if necessary, easily taken into account by means of appropriate geometrical coefficients, cf., e. g., [2]).

In this approximation, the chemical potential of adatoms in a terrace of monoatomic height can be represented as

$$\mu_a^{'} = kT\ln\left(\frac{c^*_{a,R}}{c_a^{(0)}}\right),$$

where $c^*_{a,R}$ is the equilibrium surface concentration of adatoms on the surface of a particle of radius $R$, resulting in

$$\Delta\mu_a = \mu_a - \mu_a^{'} = kT\ln\alpha_R,$$

where

$$\alpha_R = \frac{\overline{c}_a}{c^*_{a,R}}, \tag{11}$$

replacing in Eq. (5) the saturation ratio $\alpha = \overline{c}_a/c^*_a$ defined in Eq. (9).

Furthermore, the area of the terrace and its perimeter are calculated as

$$S_t = 2\pi R^2(1-\cos\varphi)$$

and

$$L_t = 2\pi R\sin\varphi,$$

respectively, where $0 \le \varphi \le \pi$ is the angle defined in Fig. 1, and thus the free energy of terrace formation instead of Eq. (5) takes the form

$$\Delta G_R(\varphi) = -\frac{S_t}{s}\left(\mu_a - \mu_a^{'}\right) + L_t\lambda = \\ = -\frac{2\pi R^2 a}{\Omega}(1-\cos\varphi)\,kT\ln\alpha_R + 2\pi R\lambda\sin\varphi. \tag{12}$$

The radius of the critical terrace is calculated as

$$\rho^* = R\sin\varphi^*, \tag{13}$$

where the critical angle $\varphi^*$ is determined from the condition,

$$\frac{d\Delta G(\varphi)}{d\varphi} = 0,$$

as

$$\mathrm{tg}\,\varphi^*(R) = \frac{\lambda\Omega}{RakT\ln\alpha_R}. \tag{14}$$

In particular, for the critical particle of radius $R^*$ that is in equilibrium with the melt (considered below in Section 4), i. e., $c^*_{a,R^*} = \overline{c}_a$ and $\alpha_{R^*} = 1$, this gives

$$\varphi^*(R^*) = \frac{\pi}{2}. \tag{15}$$

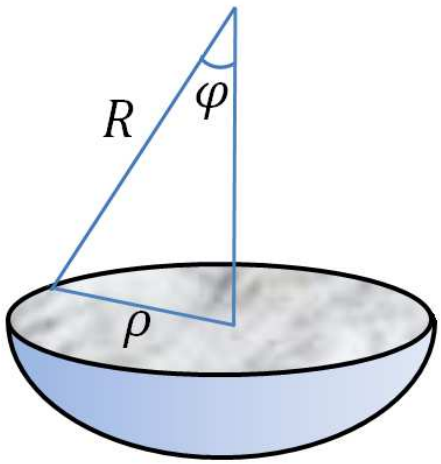


**Fig. 1.** Terrace geometry on the surface of a spherical particle of radius $R$

This result has a clear physical meaning: for a critical particle that is in equilibrium with the melt, i. e.,

$$\Delta\mu_a = \mu_a - \mu_a^{'} = kT \ln \alpha_{R^*} = 0,$$

the free energy of terrace formation is completely determined by the terrace perimeter,

$$\Delta G_{R^*}(\varphi) = L_t = 2\pi R^* \lambda \sin\varphi,$$

which has a maximum at the equator of the particle.

Substitution of Eq. (14) into Eq. (13) results in

$$\rho^* = \frac{R\lambda\Omega}{\left[(RakT\ln\alpha_R)^2 + (\lambda\Omega)^2\right]^{1/2}}, \qquad (16)$$

which, for a particle in a small vicinity of the critical size, $R \to R^*$ (and thus $\alpha_R \to 1$), gives $\rho^* \to R$.

It is important to note that atomic terraces can nucleate on the surface of both supercritical and subcritical particles, i. e., either for $\alpha_R > 1$ or for $\alpha_R < 1$, but with different probabilities. Indeed, in both cases $\Delta G_R(\varphi)$ has a maximum at $\varphi^*(R)$, which defines the nucleation barrier calculated by substituting Eqs (13) and (14) into Eq. (12) as

$$\Delta G_R(\varphi^*) = -\frac{2\pi R^2 akT\ln\alpha_R}{\Omega} \times \left[1 - \frac{RakT\ln\alpha_R}{\left[(\lambda\Omega)^2 + (RakT\ln\alpha_R)^2\right]^{1/2}}\right] + \frac{2\pi R\lambda^2\Omega}{\left[(\lambda\Omega)^2 + (RakT\ln\alpha_R)^2\right]^{1/2}}, \qquad (17)$$

which for particles in a small vicinity of the critical size, $R \approx R^*$ (where $\ln\alpha_R \to 0$), is reduced to

$$\Delta G_R(\varphi^*) \approx -\frac{2\pi R^2 a}{\Omega} kT\ln\alpha_R + 2\pi R\lambda, \qquad (18)$$

which is slightly different for $R > R^*$ and for $R < R^*$.

The Zeldovich factor is calculated from Eq. (4) (given that $\sin\varphi^* > 0$) as

$$Z = \left[\frac{1}{2\pi kT}(\sin\varphi^*)^{-3}\frac{\lambda\Omega^2}{2\pi R^3 a^2}\right]^{1/2}, \qquad (19)$$

which for particles in the vicinity of the critical size, $R \approx R^*$ (where $\sin\varphi^* \approx 1$), is reduced to

$$Z \approx \frac{\Omega}{2\pi a}\left(\frac{\lambda}{kTR^3}\right)^{1/2}. \qquad (20)$$

Applying Eq. (10) to $L \approx 2R$, the arrival rate of adatoms to the critical terrace can be estimated as

$$\omega_a^*(R) = \omega_a(\rho^*(R)) \approx \frac{2\pi\overline{c}_a D_s a}{\Omega\Gamma}, \qquad (21)$$

where $\Gamma \approx \ln(2R/\rho^*)$. In this (logarithmic) approximation, for particles in the vicinity of the critical size, $R \approx R^*$ (where $\rho^* \to R$, as explained above, and thus $\Gamma \approx 1$), Eq. (21) can be further simplified using Eq. (9) as

$$\omega_a^*(R \approx R^*) \approx \frac{2\pi a}{\Omega} c_a^* D_s \exp\left(\frac{\Delta g}{kT}\right). \qquad (22)$$

More generally, this theory should be extended by additional consideration of vacancies in the surface monolayer ($V$) with the chemical potential $\mu_v$, which are in equilibrium with adatoms ($A$) with respect to the formation/annihilation reactions $V + A \leftrightarrow 0$, or $\mu_v = -\mu_a$ (including also their values at saturation, $\mu_v^{'} = -\mu_a^{'}$). In this case, the agglomeration of $n_a$ adatoms and $n_v$ surface vacancies into a terrace of size $n = n_a - n_v$ decreases the free energy of the system by

$$n_a\left(\mu_a - \mu_a^{'}\right) + n_v\left(\mu_v - \mu_v^{'}\right) = (n_a - n_v)\left(\mu_a - \mu_a^{'}\right) = n\left(\mu_a - \mu_a^{'}\right),$$

which is the first (negative) term in Eq. (12), and increases the free energy by the linear energy of the terrace, which is the second (positive) term in Eq. (12).

In this case, the contribution of the arrival rates of both adatoms and surface vacancies should be taken into account in Eq. (22), leading to $\omega^* = \omega_a^* + \omega_v^*$ (see details below in Section 3). However, for simplicity, we will assume that one type of these defects dominates,

e. g., $\omega_v^* \ll \omega_a^*$ (to be consistent with Pound and Hirth' theory using Eq. (8)), and so we will further assume that the mass transfer at the particle surface is provided by adatoms, $\omega^* \approx \omega_a^*$ (which in the reverse case, $\omega_a^* \ll \omega_v^*$, turns into $\omega^* \approx \omega_v^*$).

Substituting Eqs (18), (20) and (22) into Eq. (3) (given $N_1 = \overline{c}_a a\Omega^{-1}$) leads to an expression for the nucleation rate of terraces (number per unit square per unit time), which for particles in the vicinity of the critical size, $R \approx R^*$, is reduced to

$$\dot{N}_t \approx c_a^{*2} \frac{D_s a}{R^{3/2}\Omega} \left(\frac{\lambda}{kT}\right)^{1/2} \times \times \exp\left(\frac{2\pi R^2 a \ln\alpha_R}{\Omega} - \frac{2\pi R\lambda}{kT} + \frac{2\Delta g}{kT}\right). \quad (23)$$

## 3. GROWTH AND DISSOLUTION OF PARTICLES WITH $R \approx R^*$

As explained in Section 1, the growth of an atomically smooth interface is strongly suppressed [7], and can occur as a result of the formation of two-dimensional nuclei (terraces) as sources of growth layers. Accordingly, the particle growth rate is controlled by the rates of nucleation and (diffusion) growth of terraces on its faces.

In addition, it should be taken into account that for $R \approx R^*$ void terraces nucleate competitively with respect to the atomic terraces, and hence can further suppress the growth of supercritical particles.

Indeed, the change in the chemical potential of surface vacancies due to agglomeration into a disc-shaped void terrace in the surface monolayer is equal to $\Delta\mu_v = kT\ln\alpha_R$ (see Section 2.2 above), which becomes positive for supercritical particles (with $R > R^*$) and negative for subcritical particles (with $R < R^*$). Accordingly, the free energy of void terrace formation takes the form

$$\Delta G_R^{(v)}(\varphi) = \frac{2\pi R^2 a}{\Omega}(1-\cos\varphi)\, kT\ln\alpha_R + 2\pi R\lambda\sin\varphi. \quad (24)$$

where the first term has the opposite sign compared to Eq. (12), while the second term describing the linear energy of the void terrace edge (characterised by the same value of $\lambda$), is not changed.

Since the mass transfer on the particle surface is carried out by the same type of surface point defects, e. g., by adatoms (as assumed above in Section 2.2), the kinetic factor $\omega^*$ in the expression for the nucleation rate of a void terrace, Eq. (3), is equal to the arrival rate of adatoms to the critical terrace $\omega_a(n^*)$.

Indeed, in a small vicinity of the critical vacancy cluster size, $n \approx n^*$, the kinetic factor $\omega$ is calculated from the general relationship of Zeldovich's theory [5] (see also [25])

$$\omega = -kT\left(\frac{dn}{dt}\right)\left(\frac{d\Delta G_R^{(v)}}{dn}\right)^{-1}, \quad (25)$$

where $\left(\frac{dn}{dt}\right)$ is the 'macroscopic' growth rate of the supercritical vacancy cluster, expressed as

$$\left(\frac{dn}{dt}\right) = \omega_v(n) - \zeta_v(n) - \omega_a(n) + \zeta_a(n), \quad (26)$$

where $\omega_{v(a)}$ and $\zeta_{v(a)}$ are, respectively, the arrival and emission rates of vacancies (adatoms) to (from) the terrace, related by the Gibbs – Kelvin equilibrium condition as

$$\zeta_v = \omega_v \exp\left(\frac{1}{kT}\frac{\partial\Delta G_R^{(v)}}{\partial n_v}\right) = \omega_v \exp\left(\frac{1}{kT}\frac{d\Delta G_R^{(v)}}{dn}\right), \quad (27)$$

and

$$\zeta_a = \omega_a \exp\left(\frac{1}{kT}\frac{\partial\Delta G_R^{(v)}}{\partial n_a}\right) = \omega_a \exp\left(-\frac{1}{kT}\frac{d\Delta G_R^{(v)}}{dn}\right), \quad (28)$$

taking into account that the size of the vacancy cluster, formed by the agglomeration of $n_v$ surface vacancies and $n_a$ adatoms, is equal to $n = n_v - n_a$. In the vicinity of the critical cluster size, $n \approx n^*$ (where $\frac{d\Delta G_R^{(v)}}{dn} \to 0$), Eqs (27) and (28) are reduced to

$$\zeta_{v(a)} \approx \omega_{v(a)}\left(1 \pm \frac{1}{kT}\frac{d\Delta G_R^{(v)}}{dn}\right). \quad (29)$$

Accordingly, the growth rate in Eq. (26) is calculated as

$$\left(\frac{dn}{dt}\right)_{macro} \approx -(\omega_a + \omega_v)\frac{1}{kT}\frac{d\Delta G_R^{(v)}}{dn}, \quad (30)$$

and from Eq. (25) one obtains

$$\omega^* = \omega_a^* + \omega_v^*, \quad (31)$$

which under the above assumption that mass transfer on the particle surface is provided by adatoms, $\omega_v^* \ll \omega_a^*$, is reduced to $\omega^* \approx \omega_a^*$.

Therefore, the nucleation rate of void terraces on the surface of an off-critical particle is calculated as

$$\dot{N}_{vt} \approx c_a^{*2} \frac{D_s a}{R^{3/2}\Omega} \left(\frac{\lambda}{kT}\right)^{1/2} \times \times \exp\left(-\frac{2\pi R^2 a \ln\alpha_R}{\Omega} - \frac{2\pi R\lambda}{kT} + \frac{2\Delta g}{kT}\right), \quad (32)$$

which differs from Eq. (23) for atomic terraces by the sign of the first term in the exponent.

For off-critical particles with $R \approx R^*$, corresponding to $|\alpha_R - 1| \ll 1$, the growth time of an atomic (or void) terrace (until a monolayer is formed (or disappears)) can be neglected in comparison with the inverse rate of its generation, which determines in this (so called 'mononuclear') limit the interface relocation velocity. This relocation occurs in competition between atomic and void terraces, which determines the growth rate of a particle,

$$\frac{dV_p}{dt} = \frac{dn}{dt}\Omega \approx 4\pi R^2 \left(\dot{N}_t - \dot{N}_{vt}\right)\left(\pi R^2 a\right), \qquad (33)$$

or

$$\frac{dR}{dt} \approx \pi R^2 a \left(\dot{N}_t - \dot{N}_{vt}\right), \qquad (34)$$

which after substitution of Eqs (23) and (32) takes the form

$$\frac{dV_p}{dt} \approx 8\left(\pi R^2\right)^2 c_a^{*2} \frac{D_s a^2}{R^{3/2}\Omega}\left(\frac{\lambda}{kT}\right)^{1/2} \times \\ \times \exp\left(-\frac{2\pi R\lambda}{kT} + \frac{2\Delta g}{kT}\right) \mathrm{sh}\left(\frac{2\pi R^2 a \ln\alpha_R}{\Omega}\right). \qquad (35)$$

In the considered limit $R \to R^*$ (and $\ln\alpha_R \to 0$), when

$$\mathrm{sh}\left(\frac{2\pi R^2 a \ln\alpha_R}{\Omega}\right) \approx \frac{2\pi R^2 a \ln\alpha_R}{\Omega},$$

Eq. (35) can be reduced to the expression

$$\frac{dV_p}{dt} \approx 16 R^6 \pi^3 c_a^{*2} \frac{D_s a^3}{R^{3/2}\Omega^2}\left(\frac{\lambda}{kT}\right)^{1/2} \times \\ \times \ln\alpha_R \exp\left(-\frac{2\pi R\lambda}{kT} + \frac{2\Delta g}{kT}\right), \qquad (36)$$

which describes the growth $\left(\frac{dV_p}{dt} > 0\right)$ and dissolution $\left(\frac{dV_p}{dt} < 0\right)$ of supercritical and subcritical particles, respectively, and will be used further to calculate the crystal nucleation rate.

## 4. HOMOGENEOUS NUCLEATION OF CRYSTALS WITH ATOMICALLY SMOOTH SURFACES FROM MELT

In order to calculate the nucleation rate of crystals with atomically smooth interfaces (for simplicity considering a one-component system) using classical nucleation theory, the parameters of the general expression, Eq. (3), should be evaluated. The Gibbs free energy of the formation of a (quasi-) spherical nucleus, consisting of $x$ monomers (atoms) takes the form (see, e. g., [1])

$$\Delta G_p(x) = \gamma\left(36\pi\Omega^2\right)^{1/3} x^{2/3} - kTx\ln\alpha, \qquad (37)$$

where $V_p = x\Omega$ and $R = \left(\frac{3\Omega}{4\pi}x\right)^{1/3}$ are the volume and radius of the nucleus respectively, and the parameter $\alpha$ is the supercooling ratio defined in Eq. (9). Therefore, the equilibrium condition, $\frac{d\Delta G_p(x)}{dx} = 0$, takes the form

$$kT\ln\alpha = \frac{2\gamma\Omega}{R}, \qquad (38)$$

which determines the saturation concentration of adatoms on the particle surface, $c^*_{a,R}$, as

$$kT\ln\left(\frac{c^*_{a,R}}{c^*_a}\right) = \frac{2\gamma\Omega}{R}, \qquad (39)$$

and allows calculating the parameter $\alpha_R$, defined in Eq. (11) (and used above in Section 3 to calculate the growth rate of off-critical particles), as

$$\alpha_R = \frac{\overline{c}_a}{c^*_{a,R}} = \frac{\overline{c}_a}{c^*_a}\frac{c^*_a}{c^*_{a,R}} = \alpha\frac{c^*_a}{c^*_{a,R}} = \alpha\exp\left(-\frac{2\gamma\Omega}{RkT}\right). \qquad (40)$$

The size $x^*$ (and radius $R^*$) of the critical nucleus at a given $\alpha$ is obtained from Eq. (38), applied to $R = R^*$ (for which $c^*_{a,R^*} = \overline{c}_a$),

$$kT\ln\alpha = kT\ln\left(\frac{\overline{c}_a}{c^*_a}\right) = kT\ln\left(\frac{c^*_{a,R^*}}{c^*_a}\right) = \frac{2\gamma\Omega}{R^*}, \qquad (41)$$

leading to

$$R^* = \frac{2\gamma\Omega}{kT\ln\alpha}, \qquad (42)$$

or

$$x^* = \frac{32\pi\Omega^2}{3}\left(\frac{\gamma}{kT\ln\alpha}\right)^3. \qquad (43)$$

Substitution of Eq. (41) into Eq. (40) with $R = R^*$ results consistently in $\alpha_{R^*} = 1$.

The nucleation barrier (from Eq. (3)) is calculated by substitution of Eq. (43) into Eq. (37) as

$$\Delta G^*_p = \frac{16\pi\gamma^3\Omega^2}{3(kT\ln\alpha)^2}, \qquad (44)$$

whereas the Zeldovich factor is calculated by substitution of Eq. (37) into Eq. (4) as

$$Z \approx \frac{(kT\ln\alpha)^2}{8\pi(kT)^{1/2}\gamma^{3/2}\Omega}. \qquad (45)$$

The growth rate of a particle in a small vicinity of the critical size, $R \approx R^*$, is calculated by substitution of Eq. (40) into Eq. (36) as

$$\frac{dx}{dt} = 16\pi^3 R^{9/2} c_a^{*2} \left(\frac{\lambda}{kT}\right)^{1/2} \frac{D_s a^3}{\Omega^3} \times \\ \times \left(\ln\alpha - \frac{2\gamma\Omega}{RkT}\right) \exp\left(-\frac{2\pi R\lambda}{kT} + 2\ln\alpha\right), \quad (46)$$

and, after substitution of Eqs (41), as

$$\frac{dx}{dt} = 16\pi^3 R^{9/2} c_a^{*2} \left(\frac{\lambda}{kT}\right)^{1/2} \frac{D_s a^3}{\Omega^3} \frac{2\gamma\Omega}{kT} \times \\ \times \left(\frac{1}{R^*} - \frac{1}{R}\right) \exp\left(-\frac{2\pi R\lambda}{kT} + 2\ln\alpha\right), \quad (47)$$

whereas from Eq. (37) one obtains in the same vicinity

$$\frac{d\Delta G_p(x)}{dx} = -\frac{2\gamma\Omega}{kT}\left(\frac{1}{R^*} - \frac{1}{R}\right). \quad (48)$$

Substituting Eqs (47) and (48) into the general expression of the nucleation theory (cf. Eq. (25)),

$$\omega = -kT\left(\frac{dx}{dt}\right)\left(\frac{d\Delta G_p}{dx}\right)^{-1}, \quad (49)$$

allows calculating the kinetic factor $\omega^*$ of the nucleation rate using Eq. (9) as

$$\omega^* \equiv \omega(R^*) = 16\pi^3 R^{*9/2} c_a^{*2} \left(\frac{\lambda}{kT}\right)^{1/2} \times \\ \times \frac{D_s a^3}{\Omega^3} \exp\left(-\frac{2\pi R^*\lambda}{kT} + \frac{2\Delta g}{kT}\right). \quad (50)$$

The substitution of Eqs (44), (45) and (50) into the general equation of the nucleation theory, Eq. (3), with $N_1 = \Omega^{-1}$, results in the following expression for the nucleation rate,

$$\dot{N} = \frac{32\pi^2\gamma^3(2\lambda)^{1/2}}{(kT\ln\alpha)^{5/2}} \frac{D_s a^3}{\Omega^{1/2}kT} c_a^{*2} \times \\ \times \exp\left\{-\frac{16\pi\gamma^3\Omega^2}{3(kT)^3(\ln\alpha)^2} - \frac{4\pi\lambda\gamma\Omega}{(kT)^2\ln\alpha} + \frac{2\Delta g}{kT}\right\} = \\ = \frac{16\pi^2\gamma^3(2\lambda)^{1/2}}{(\Delta g)^{5/2}} \frac{D_s a^3}{\Omega^{1/2}kT} c_a^{*2} \times \\ \times \exp\left\{-\frac{16\pi\gamma^3\Omega^2}{3kT(\Delta g)^2} - \frac{4\pi\lambda\gamma\Omega}{kT\Delta g} + \frac{2\Delta g}{kT}\right\}. \quad (51)$$

In the traditional models (discussed in Section 1), which are applicable to crystals with the atomically rough surface and for which the arrival rate to the critical nucleus is controlled by random attachment of atoms at the interface, the nucleation rate is calculated as (cf. [1])

$$\dot{N}' = \frac{24D_b}{\Omega a^2} x^{*\frac{2}{3}} \left(\frac{\Delta g}{6\pi kTx^*}\right)^{\frac{1}{2}} \exp\left[-\frac{16\pi\gamma^3\Omega^2}{3kT(\Delta g)^2}\right] = \\ = \left(\frac{32}{3}\right)^{\frac{1}{6}} \frac{24D_b\gamma^{1/2}}{6^{1/2}\pi^{1/3}\Omega^{2/3}a^2(kT)^{1/2}} \exp\left[-\frac{16\pi\gamma^3\Omega^2}{3kT(\Delta g)^2}\right], \quad (52)$$

which in the vicinity of the critical supercooling, $\alpha \approx 1$, can significantly overestimate the (governing) exponential factor, but underestimate the pre-exponential factor,

$$\frac{\dot{N}}{\dot{N}'} = \frac{4\pi^2 2^{1/6}\gamma^{5/2}\lambda^{1/2}\Omega^{1/6}}{(\Delta g)^{5/2}} \frac{D_s}{D_b} \frac{a^4}{(kT)^{1/2}} c_a^{*2} \times \\ \times \exp\left\{-\frac{4\pi\lambda\gamma\Omega}{kT\Delta g} + \frac{2\Delta g}{kT}\right\}. \quad (53)$$

The mutual compensation of these two effects is possible within some narrow range ('window') of temperatures, and thus may provide (in combination with tuning of the surface tension value) an agreement (by chance) of the traditional model predictions with observations for crystal nucleation at temperatures below the roughening transition. However, in a more general case, the traditional approach should be applied only to analysis of nucleation at temperatures above the roughening transition. In particular, it can be concluded from the present analysis that not only the growth rate but also the nucleation rate is strongly suppressed for crystals with the atomically smooth surface.

## 5. HOMOGENEOUS NUCLEATION OF CRYSTALS WITH ATOMICALLY SMOOTH SURFACES FROM AQUEOUS SOLUTION

Nucleation of crystals from aqueous solution is normally studied at constant temperature and as a function of supersaturation. For crystalline nuclei with atomically smooth surfaces, which are formed in the one-step nucleation mechanism (i. e., in the absence of pre-nucleation clusters, see Section 1) and whose growth is controlled by the mechanism of surface nucleation, the theory developed above can be modified to take into account the change in the driving force of the nucleation process in solutions. This requires redefining the parameter $\alpha$ in Eq. (9), which in this case is equal to the supersaturation ratio of the solution,

$$\alpha = \frac{\overline{c}_b}{c_b^*}, \quad (54)$$

where $\overline{c}_b$ is the concentration of solute atoms in the melt and $c_b^*$ is the saturation concentration.

The saturation concentration $c_b^*$ is related to the saturation surface concentration $c_a^*$ by the equilibrium condition,

$$kT \ln\left(\frac{c_a^*}{c_a^{(0)}}\right) = kT \ln\left(\frac{c_b^*}{c_b^{(0)}}\right),$$

where $c_a^{(0)}$ and $c_b^{(0)}$ are the thermal surface and bulk concentration, respectively, which can be presented in the form

$$c_a^* = c_b^* \frac{c_a^{(0)}}{c_b^{(0)}}. \tag{55}$$

Besides, the parameter $N_1$ in Eq. (2) (the number density of monomers in the metastable phase) in this case is equal to

$$N_1 = \overline{c}_b \Omega^{-1}, \tag{56}$$

in accordance with Frenkel's model [26] (additionally justified in the author's paper [27]).

Therefore, the nucleation rate obtained from the modified Eq. (51) takes the form

$$\dot{N} = \frac{32\pi^2\gamma^3(2\lambda)^{1/2}}{(kT\ln\alpha)^{5/2}} \frac{D_s a^3}{\Omega^{1/2} kT} \overline{c}_b^3 \left(\frac{c_a^{(0)}}{c_b^{(0)}}\right)^2 \times \exp\left\{-\frac{16\pi\gamma^3\Omega^2}{3(kT)^3(\ln\alpha)^2} - \frac{4\pi\lambda\gamma\Omega}{(kT)^2\ln\alpha}\right\}. \tag{57}$$

In the case of a two-step nucleation mechanism through an intermediate metastable phase (i. e., with a larger value of saturation concentration, $c_b^{*'} > c_b^*$), the nucleation of metastable phase occurs at $\overline{c}_b > c_b^{*'}$ and may dominate over the nucleation of the crystalline phase due to the lower surface tension $\gamma'$ of the metastable phase, $\gamma' < \gamma$, which may lower the nucleation barrier of this phase compared to the crystalline phase under the approximate condition (neglecting the contribution of pre-exponential factors),

$$\frac{16\pi\gamma'^3\Omega^2}{3(kT)^3(\ln\alpha')^2} < \frac{16\pi\gamma^3\Omega^2}{3(kT)^3(\ln\alpha)^2} + \frac{4\pi\lambda\gamma\Omega}{(kT)^2\ln\alpha}, \tag{58}$$

where $\alpha' = \frac{\overline{c}_b}{c_b^{*'}} > 1$ (cf. [28]).

In this case, Eq. (57) is applicable in a relatively narrow range of concentrations above the saturation point, $c_b^* < \overline{c}_b < c_b^{*'}$, in which direct nucleation of crystalline particles occurs (albeit at a reduced rate corresponding to the small values of $\alpha$ in the exponent of Eq. (57)).

## 6. OSTWALD RIPENING OF CRYSTALLINE PARTICLES IN SOLUTIONS

Although nucleation by a one-step mechanism (i. e., by direct formation of crystalline nuclei) can be suppressed in aqueous solutions (as discussed in Section 1), the faceted structure of crystalline particles is well-formed at later stages of precipitation. Therefore, the growth of crystalline particles, which is controlled by 2D nucleation, in the vicinity of the critical radius $R^*$ is described by the rate equation, Eq. (47), which, after substituting Eqs (54) and (55), takes the form

$$\frac{dR}{dt} = 4\pi^2 R^{3/2} \left(\overline{c}_b \frac{c_a^{(0)}}{c_b^{(0)}}\right)^2 \left(\frac{\lambda}{kT}\right)^{1/2} \frac{D_s a^3}{\Omega} \frac{2\gamma}{kT} \times \times \frac{(R-R^*)}{R^*} \exp\left(-\frac{2\pi R\lambda}{kT}\right). \tag{59}$$

This equation is more complicated than the growth rate equations for precipitates with atomically rough surfaces used to analyse Ostwald ripening by Lifshitz and Slyozov [29] and Wagner [30]. For this reason, the late stage of precipitation (when supersaturation becomes very low) cannot be rigorously studied within an analytical approach (and requires numerical calculations).

Instead, a simplified analysis can be performed for the upper limit of the growth rate to demonstrate the extremely slow precipitation kinetics of crystalline particles at the late stage. For this purpose, the growth rate equation, Eq. (59), will be analysed for a particle of radius $R(t)$, which at $t \to \infty$ is approaching the critical radius $R^*(t)$ but is still larger, obeying the condition $R(t) - R^*(t) < R^*(t)$. Considering that the size distribution function should narrow with time (based on the results of Lifshitz – Slyozov – Wagner (LSW) theory for simpler cases and available experimental observations discussed below) and that the critical radius is inside this size distribution (providing growth of supercritical particles at expense of subcritical ones), this analysis becomes representative of particles that have survived the Ostwald ripening stage.

In this approach, the upper limit for the growth rate can be evaluated, using Eq. (59), in terms of the particle dimensionless radius

$$\rho(t) = \frac{2\pi\lambda}{kT} R(t)$$

as

$$\frac{d\rho}{dt} < 8\pi^2 \left(\overline{c}_b \frac{c_a^{(0)}}{c_b^{(0)}}\right)^2 \frac{D_s a^3 \gamma}{\Omega kT} \rho^{\frac{3}{2}} \exp(-\rho), \tag{60}$$

so that $\rho(t)$ is bounded, $\rho(t) < \widetilde{\rho}(t)$, by the solution $\widetilde{\rho}(t)$ of the equation

$$\rho^{-\frac{3}{2}} e^{\rho} \frac{d\rho}{dt} = 8\pi^2 \left( \overline{c}_b \frac{c_a^{(0)}}{c_b^{(0)}} \right)^2 \frac{D_s a^3 \gamma}{\Omega k T}, \qquad (61)$$

which can be integrated as

$$e^{\widetilde{\rho}} \left[ 2F\left( \widetilde{\rho}^{\frac{1}{2}} \right) - \widetilde{\rho}^{\frac{1}{2}} \right] = 4\pi^2 \left( \overline{c}_b \frac{c_a^{(0)}}{c_b^{(0)}} \right)^2 \frac{D_s a^3 \gamma}{\Omega k T} t, \qquad (62)$$

where

$$F(x) \equiv e^{-x^2} \int_0^x e^{y^2} dy$$

is Dawson's integral.

The asymptotic solution of Eq. (62) at $t \to \infty$ (when $\widetilde{\rho} \to \infty$ and $F(\widetilde{\rho}) \to 2\widetilde{\rho}^{-1} + 4\widetilde{\rho}^{-3} + \ldots$) takes the form

$$\widetilde{\rho}^{-\frac{3}{2}} e^{\widetilde{\rho}} = 16\pi^2 \left( \overline{c}_b \frac{c_a^{(0)}}{c_b^{(0)}} \right)^2 \frac{D_s a^3 \gamma}{\Omega k T} t, \qquad (63)$$

or, since $\widetilde{\rho} \gg 2 \ln \widetilde{\rho}$ at $\widetilde{\rho} \gg 1$, one can derive with good accuracy

$$R(t) < \widetilde{R}(t) \sim \frac{kT}{2\pi\lambda} \ln t. \qquad (64)$$

This result is in qualitative agreement with experimental observations of Ostwald ripening of quartz in a hydrous silicic melt [31], which proceeded very sluggishly, and the mean grain size of quartz was well fitted by a logarithmic law, $\sim \ln t$. It was observed that the precipitating quartz crystals have flat, crystallographically controlled faces, so it was assumed that they grow by a layer growth mechanism controlled by 2D nucleation (which was also assumed above in the derivation of Eq. (59)). These experimental results have been extrapolated to geological time scales leading to the conclusion that Ostwald ripening cannot have any significant effect in natural quartz-bearing magmatic systems, and therefore the correct interpretation of these results by theory may have practical importance.

## 7. CONCLUSIONS

A new model for the kinetics of homogeneous nucleation of crystals from melts is developed in the framework of classical nucleation theory. The traditional approach considering the mechanism of mass transfer from the melt to nucleated particles by random attachment of atoms at the interface, which is valid for crystals with atomically rough interface, is modified in application to faceted crystalline particles with atomically smooth interface, whose growth is controlled by two-dimensional nucleation of terraces of monoatomic height on crystal faces.

Taking into account that the growth rate of a given face for a perfect crystal must show a discontinuity at its roughening temperature and that the melting point in many materials is reached before the roughening transition of the plane facets, it is assumed that nucleation in melts may occur by formation of crystalline particles with atomically smooth interface. This assumption is supported by MD simulations from the literature for nucleation in melts of various crystalline materials including Mo [14], Al [15] and NaCl [16], showing that small nanometre-sized particles formed during nucleation have the crystalline structure of bulk material and are clearly faceted.

Although experimental methods that can detect nucleation and the formation of the crystal (predominantly by means of optical microscopy) generally do not provide any microscopic detail on the structure of nucleated crystalline phase, some observations (e. g., nucleation in alkali halide melts [18]) support the conclusion concerning the crystalline structure of nuclei. Based on these observations, it was concluded that classical nucleation theory should be modified to take into account the three-dimensional crystal structure of nuclei, which are bounded by perfectly close-packed planes and whose growth can only occur by repeated two-dimensional nucleation of fresh surface layers [18].

The development of such a model for nucleation in melts is performed in the present work, which demonstrates a strong suppression of the nucleation rate compared to the traditional approach (applicable to nuclei with rough surfaces). For nucleation in aqueous solutions, which, presumably because of the strong influence of water molecules on the atomic structure of nuclei [17], can proceed through an intermediate metastable phase (i. e., with a larger value of the saturation concentration) in accordance with the so-called two-step nucleation mechanism, the new model can be used only in a relatively narrow concentration range between the two saturation concentrations.

Although nucleation by a one-step mechanism (i. e., by direct formation of crystalline nuclei) can be suppressed in aqueous solutions, the faceted structure of crystalline particles is well-formed at later stages of precipitation. Therefore, the growth of crystalline particles, which is controlled by 2D nucleation, in the vicinity of the critical radius $R^*$ can be described by the new model applied to the Ostwald ripening stage, in

which supercritical particles grow mainly due to the dissolution of subcritical ones. Due to the complexity of the obtained growth rate equation at the late stage of precipitation, they cannot be rigorously studied in the framework of the analytical approach (used in the Lifshitz – Slyozov – Wagner theory [29, 30]). Instead, a simplified analysis can be performed for the upper limit of the growth rate to demonstrate the extremely slow precipitation kinetics of crystalline particles, $\sim \ln t$, at the late stage. The result of this analysis is in qualitative agreement with experimental observations of Ostwald ripening of quartz in a hydrous silicic melt [31], which proceeded very slowly and the mean grain size of quartz was well fitted by a logarithmic law.

**Acknowledgements.** Dr. V. Tarasov (IBRAE, Moscow) is greatly acknowledged for critical reading of the manuscript and valuable comments.

## REFERENCES

**1**. K. F. Kelton and A. L. Greer, *Nucleation in Condensed Matter: Applications in Materials and Biology, Vol. 15*, Elsevier (2010).

**2**. A. A. Chernov, *Modern Crystallography Iii: Crystal Growth, Vol. 36*, Springer Science and Business Media (2012).

**3**. M. Volmer and A. Weber, *Keimbildung in Ubersattigten Gebilden*, Z. Phys. Chem. **119**, 277 (1926).

**4**. R. Becker and W. Doering, *Kinetische Behandlung der Keimbildung in Ubersattigten Dampfen*, Ann. Phys. **24**, 719 (1935).

**5**. Ya. B. Zeldovich, *On the Theory of New Phase Formation: Cavitation*, Acta Physicochim. URSS **18**, 1 (1943).

**6**. D. Turnbull and J. C. Fisher, *Rate of Nucleation in Condensed Systems*, J. Chem. Phys. **17**, 71 (1949).

**7**. W. K. Burton, N. Cabrera, and F. C. Frank, *The Growth of Crystals and the Equilibrium Structure of Their Surfaces*, Philosophical Transactions of the Royal Society of London. Series A, Mathematical and Physical Sciences **243**, 299 (1951).

**8**. A. Pavlovska and D. Nenow, *Experimental Study of the Surface Melting of Tetrabrommethane*, J. Crystal Growth **39**, 346 (1977).

**9**. K. A. Jackson and C. E. Miller, *Experimental Observation of the Surface Roughening Transition in Vapor Phase Growth*, J. Crystal Growth **40**, 169 (1977).

**10**. B. E. Sundquist, *A Direct Determination of the Anisotropy of the Surface Free Energy of Solid Gold, Silver, Copper, Nickel, and Alpha and Gamma Iron*, Acta Metallurgica **12**, 67 (1964).

**11**. H. Muller-Krumbhaar, in: *Crystal Growth and Materials*, ed. by E. Kaldis and H. J. Scheel, North-Holland, Amsterdam (1977), p. 115.

**12**. J. C. Heyraud and J. J. Metois, *Growth Shapes of Metallic Crystals and Roughening Transition*, J. Crystal Growth **82**, 269 (1987).

**13**. G. C. Sosso, J. Chen, S. J. Cox, M. Fitzner, P. Pedevilla, A. Zen, and A. Michaelides, *Crystal Nucleation in Liquids: Open Questions and Future Challenges in Molecular Dynamics Simulations*, Chem. Rev. **116**, 7078 (2016).

**14**. Y. Shibuta, *A Molecular Dynamics Study of Effects of Size and Cooling Rate on the Structure of Molybdenum Nanoparticles*, J. Thermal Sci. Technol. **7**, 45 (2012).

**15**. A. Mahata, M. A. Zaeem, and M. I. Baskes, *Understanding Homogeneous Nucleation in Solidification of Aluminum by Molecular Dynamics Simulations*, Modelling and Simulation in Materials Science and Engineering **26**, 025007 (2018).

**16**. C. Valeriani, E. Sanz, and D. Frenkel, *Rate of Homogeneous Crystal Nucleation in Molten NaCl*, J. Chem. Phys. **122**, 194501 (2005).

**17**. D. Chakraborty and G. N. Patey, *How Crystals Nucleate and Grow in Aqueous NaCl Solution*, J. Phys. Chem. Lett. **4**, 573 (2013).

**18**. E. R. Buckle and A. R. J. P. Ubbelohde, *Studies on the Freezing of Pure Liquids I. Critical Supercooling in Molten Alkali Halides*, Proc. Royal Society of London. Series A. Mathematical and Physical Sciences **259**, 325 (1960).

**19**. G. M. Pound, M. T. Simnad, and L. Yang, *Heterogeneous Nucleation of Crystals From Vapor*, J. Chem. Phys. **22**, 1215 (1954).

**20**. J. P. Hirth, *On Two Dimensional Nucleation*, Acta Met. **7**, 755 (1959).

**21**. N. Cabrera and W. K. Burton, *Crystal Growth and Surface Structure. Part II*, Discussions of the Faraday Society **5**, 40 (1949).

**22**. M. S. Veshchunov, *On the Theory of Two-Dimensional Homogeneous Nucleation on Close-Packed Faces of Crystals Growing From Vapour*, Zh. Eksp. Teor. Fiz. **160**, 520 (2021) [JETP **133**, 449 (2021)].

**23**. R. J. Hunter, *Introduction to Modern Colloid Science*, Oxford University Press (1993).

**24**. U. Landman, R. N. Barnett, C. L. Cleveland, and R. H. Rast, *Theoretical Considerations of Energetics, Dynamics, and Structure at Interfaces*, J. Vacuum Sci. Technol. A: Vacuum, Surfaces, and Films **3**, 1574 (1985).

**25**. L. D. Landau and E. M. Lifshitz, *Theoretical Physics. Vol. 10. Physical Kinetics*, Elsevier, Amsterdam (1981), Chapter 99.

**26**. J. Frenkel, *Kinetic Theory of Liquids*, Dover Publication, New York (1955).

**27**. M. S. Veshchunov, *On the Theory of Nucleation of Coherent Inclusions in Irradiated Crystals*, J. Nucl. Mater. **599**, 155254 (2024).

**28**. D. Gebauer, M. Kellermeier, J. D. Gale, L. Bergstrom, and H. Colfen, *Pre-Nucleation Clusters as Solute Precursors in Crystallisation*, Chemical Society Reviews **43**, 2348 (2014).

**29**. I. M. Lifshitz and V. V. Slyozov, *The Kinetics of Precipitation From Supersaturated Solid Solution*, J. Phys. Chem. Solids **19**, 35 (1961).

**30**. C. Wagner, *Theory of Precipitate Change by Redissolution*, Z. Electrochem. **65**, 581 (1961).

**31**. H. Cabane, D. Laporte, and A. Provost, *Experimental Investigation of the Kinetics of Ostwald Ripening of Quartz in Silicic Melts*, Contributions to Mineralogy and Petrology **142**, 361 (2001).